*Published in : GeroScience (2025)*
*DOI: 10.1007/s11357-025-01974-2*
*Status : Postprint (Author's version)*

# DIURNAL DYNAMICS OF MULTILAYER BRAIN NETWORKS PREDICT COGNITIVE TRAJECTORIES IN AGING

Kenza Bennis · Anna Canal-Garcia · Joana B. Pereira · Giovanni Volpe · Francis Eustache · Christophe Phillips · Christine Bastin · Fabienne Collette · Gilles Vandewalle · Thomas Hinault

*K. Bennis · F. Eustache · T. Hinault,*
*Inserm, U1077, EPHE, UNICAEN, Normandie Université, PSL Université Paris, CHU de Caen, GIP Cyceron, Neuropsychologie Et Imagerie de La Mémoire Humaine (NIMH), Caen 14000, France*

*A. Canal-Garcia · J. B. Pereira,*
*Department of Clinical Neuroscience, Karolinska Institutet, Stockholm, Sweden*

*G. Volpe,*
*Department of Physics, University of Gothenburg, Gothenburg, Sweden*

*C. Phillips · C. Bastin · F. Collette · G. Vandewalle,*
*GIGA-CRC-Human Imaging, Université de Liège and Belgian National Fund for Scientific Research, Liège, Belgium*

**Keywords:**

Multilayer · Integration · Recruitment · RsFC · Diurnal rhythms · Cognitive aging · Brain oscillations · Circadian

**Abstract**

Resting-state functional connectivity (rsFC) is a highly dynamic process that varies across different times of the day within each individual. Although this variability was long considered to be noise, recent evidence suggests it may allow for an optimal adaptation to changes in the environment. However, the way rsFC is shaped on a circadian scale and its association with cognition are still unclear. We analyzed data from 90 late middle-aged participants from the Cognitive Fitness in Aging study (61 women; 50–69 years). Participants completed five electroencephalographic (EEG) recordings of spontaneous resting-state activity spread over 20 h of prolonged wakefulness. Using a temporal multilayer network approach, we characterized the diurnal variations of the dynamic recruitment and integration of resting-state brain networks. We focused on the theta and gamma frequency bands within the default mode network (DMN), central executive network (CEN), and salience network (SN). Additionally, we investigated the relationship between the recruitment and integration of these networks with baseline cognitive performance and at a 7-year longitudinal follow-up, as well as with positron emission tomography (PET) early neuropathological markers of Alzheimer's disease such as β-amyloid and tau/neuroinflammation. Diurnal changes in theta and gamma dynamics were associated with distinct cognitive aspects. Specifically, higher baseline memory performance was associated with higher theta dynamic integration of the SN and the CEN, as well as higher theta

*Published in : GeroScience (2025)*
*DOI: 10.1007/s11357-025-01974-2*
*Status : Postprint (Author's version)*

dynamic recruitment of the DMN. Moreover, lower longitudinal memory decline at 7 years was associated with higher theta dynamic integration of the SN, CEN, and DMN. In contrast, higher gamma diurnal dynamic integration of the SN and the CEN was associated with lower executive and attentional performance, as well as higher early β-amyloid accumulation, at baseline. These findings suggest that maintaining a balance between network flexibility and stability throughout the diurnal phase of the circadian cycle may play a crucial role in cognitive aging, with stable theta-band connectivity supporting memory, whereas excessive gamma-band stability in the SN and CEN may contribute to executive decline and early amyloid accumulation. These insights highlight the importance of considering time-of-day in brain rsFC studies, calling for a temporal multilayer approach to capture these dynamic patterns more effectively.

# Introduction

One of the major challenges of cognitive neuroscience is to understand the functional organization of the brain underlying human cognitive abilities and behaviors. Beyond brain activations, brain networks are key to the organization of cognitive abilities [14, 58]. A functional brain network can be defined as a system composed of brain regions that are more functionally connected to each other within the system than to the other regions of the brain, a property referred to as network recruitment. At the same time, brain networks are part of a highly integrated large-scale network where between-network interactions, referred to as network integration, play a key role in orchestrating complex cognitive processes. Resting-state functional connectivity (rsFC) analyses of brain signal are considered to reflect the stable and intrinsic organization of brain networks that can be related to cognition [80, 84]. Most of these studies have analyzed rsFC in isolation and averaged over entire recording sessions (or scan), implicitly assuming that brain networks' organization remains stable over space and time [6, 12]. However, accumulating evidence suggests that brain networks continuously fluctuate, requiring a more dynamic perspective.

In fact, rsFC is inherently dynamic, fluctuating both over short and long timescales, ranging from moment-to-moment switching of brain regions' connectivity patterns among various functional brain networks to slow age-related reorganization. Together, these dynamic phenomena have proven promising in finding determinants of cognitive trajectories in aging [73]. At the level of a single scan, short-term fluctuations in rsFC, particularly the frequency with which brain regions switch between different networks, have been shown to predict cognitive performance [66]. At the longest timescale, across the lifespan, rsFC undergoes gradual reorganization, reflecting compensatory mechanisms that sustain cognitive function despite age-related non-lesional changes. In particular, it has been shown that a hallmark of aging is increased integration and decreased recruitment of brain networks' rsFC associated with preserved cognitive performance. This indicates a shift toward a more distributed network organization and reduced functional specialization of brain networks to maintain cognitive performance [37, 87]. However, because these slow changes accumulate over years, they cannot directly capture the ongoing neural dynamics underlying cognitive variability [42]. Between these two extremes, an intermediate timescale exists: the diurnal phase of the circadian cycle, which refers specifically to the waking daytime phase of the circadian cycle [46].

*Published in : GeroScience (2025)*
*DOI: 10.1007/s11357-025-01974-2*
*Status : Postprint (Author's version)*

Here, we investigate age-related brain changes associated with diurnal changes in brain networks dynamics at rest. Unlike aging-related changes, diurnal fluctuations occur within hours and can be directly measured, offering a unique opportunity to examine the temporal organization of rsFC associated with the large heterogeneity of individual cognitive trajectories observed during aging [1], [11]. The rsFC signals follow structured variations across the day, shaped by the interplay between prior sleep-wake history, which sets the need for sleep, and the circadian system, which promotes wakefulness and cognition during the day while favoring sleep at night [32, 51]. However, the diurnal rsFC fluctuations in cognitive aging remain largely unexplored. In a first step toward understanding diurnal rsFC fluctuations, we previously used electroencephalography (EEG) to investigate how rsFC varies across five different times of the day (five EEG sessions), and how these fluctuations relate to cognition and tau and β-amyloid biomarkers in healthy late middle-aged participants [9]. EEG time-frequency analyses, with its millisecond-level temporal resolution, are uniquely suited to capture subtle changes in spontaneous neural dynamics over time and detect early signs of age-related cognitive decline [20]. For each session, we measured rsFC as the synchronization of brain rhythm between brain regions, with each rhythm associated with different cognitive processes and defined by its corresponding frequency band, from the slowest to the fastest rhythm: delta (1–4 Hz), theta (4–8 Hz), alpha (8–12 Hz), beta (13–30 Hz), and gamma (30–100 Hz). To quantify diurnal rsFC fluctuations, we computed a global fluctuation index across all five sessions. Among the key findings, we observed that greater diurnal rsFC fluctuations in the theta band were associated with poorer memory performance and higher tau/neuroinflammation levels, whereas greater diurnal rsFC fluctuations in the gamma band correlated with better executive function and lower β-amyloid deposition. Couplings involved in these associations were part of the salience network (SN) and the central executive network (CEN). While this previous work highlighted that diurnal rsFC fluctuations in the theta and gamma bands may reflect critical processes underlying cognitive aging, it did not capture the specific mechanisms of network reorganization, nor did it consider longitudinal cognitive trajectories.

Here, to address these gaps, we applied multilayer network analyses, a method well-suited for capturing rsFC dynamics over time [60]. In this approach, each layer represents a time-specific rsFC pattern, forming a time-varying functional network that models the continuous reorganization of brain connectivity [75]. Unlike classical methods, this framework allows us to differentiate dynamic recruitment (the stability of functional associations within a network), from dynamic integration (the extent to which regions switch between networks over time) [54]. We investigated how these dynamics relate to 6- to 7-year longitudinal cognitive trajectories and tau/β-amyloid biomarkers in healthy late middle-aged adults. Specifically, we examined SN, CEN, and DMN recruitment and integration across the day, as these networks play a central role in cognition and aging-related changes [55], [47]. We expected increased integration relative to recruitment, indicating reduced functional specialization throughout the day.

We further explored how diurnal patterns of recruitment and integration relate to cognitive trajectories and pathological markers. In the theta band, we hypothesized that greater dynamic integration would be linked to better cognitive performance, slower cognitive decline, and lower tau/neuroinflammation, reflecting preserved brain efficiency. In contrast, in the gamma band, we expected that greater dynamic integration would be associated with poorer cognitive performance, greater decline, and higher β-amyloid levels, suggesting a maladaptive process. Given that participants

*Published in : GeroScience (2025)*
*DOI: 10.1007/s11357-025-01974-2*
*Status : Postprint (Author's version)*

showed no marked cognitive deterioration, these associations may reflect early compensatory mechanisms in healthy aging preceding pathological deposition.

# Methods

## PARTICIPANTS

Participants were enrolled in a multimodal longitudinal study designed to identify cerebral biomarkers of normal cognitive aging (the Cognitive Fitness in Aging – COFITAGE – study; [86]). We analyzed data from ninety healthy late middle-aged participants (61 women and 29 men, aged 50–69 years), with EEG data recorded for all five sessions. Based on previous work investigating aging effects on oscillatory activity, a sample size of ninety participants would provide 90% power to detect an effect size of Cohen's $f$ = 0.14 (medium effect size), with an alpha = 0.05 [38]. No participants reported any recent history of neurological or psychiatric disease or were taking medication affecting the central nervous system. All participants had anatomically normal MRI scans, with no significant gray or white matter abnormalities. Extended information about protocol, exclusion criteria, recruitment, consent, and financial reward can be found in previous publications from this cohort (first in [9, 18, 19, 62, 71, 85, 86]). A subsample of 64 participants who had data for tau/neuroinflammation-PET imaging was also considered for additional analyses. After a 7-year follow-up, 58 participants were seen again for a similar neuropsychological assessment. Demographic characteristics of the final samples at baseline and after the 7-year follow-up are described in **Table 1**. The study was approved by the Medicine Faculty/Hospital Ethics Committee of the University of Liège, Belgium.

## WAKE-EXTENSION PROTOCOL

Five EEG recordings of spontaneous resting-state activity were performed over the course of 15 h, between 10 a.m. and 1 a.m. in the context of a wake-extension protocol. Participants were required to follow a regular sleep-wake schedule (± 30 min) for 1 week based on their preferred bed and wake-up times prior to the study, in order to ensure standardized baseline conditions and minimize the impact of sleep variability on cognitive measures. Compliance was verified using sleep diaries and wrist actigraphy (Actiwatch, Cambridge Neurotechnology). The day before, participants arrived at the laboratory 8 h before their habitual bedtime and were kept in dim light (< 5 lx) for 6.5 h preceding bedtime. Following the baseline night of sleep, the wake-extension protocol consisted of 20 h of continuous wakefulness under strictly controlled constant routine conditions, (i.e., in-bed semi-recumbent position, dim light < 5 lx, temperature ~19 °C, regular isocaloric food intake, no time-of-day information, and sound-proofed rooms) to counteract the effect of external influences on endogenous circadian rhythms, assessed with salivary melatonin. Under these conditions, the recordings specifically captured dynamics across the diurnal phase of the circadian cycle [46]. The time of all procedures of the wake-extension protocol was adjusted according to the clock time of the participants' habitual sleep-wake schedule. At baseline, neuropsychological assessment, β-amyloid-PET, and Tau/neuroinflammation-PET imaging together with T1-weighted MRI were also acquired on separate visits. Only neuropsychological assessment was re-performed after 7-year follow-up (**Fig. 1**A).

*Published in : GeroScience (2025)*
*DOI: 10.1007/s11357-025-01974-2*
*Status : Postprint (Author's version)*

**Table 1** Demographic, cognitive, neuroimaging, and biomarker characteristics at baseline and 7-year follow-up

| | Baseline | 7-year follow-up |
|---|---|---|
| NEUROPSYCHOLOGICAL ASSESSMENT NUMBER OF PARTICIPANTS | 90 | 58 |
| NUMBER OF FEMALES, *N* (%) | 60 (66.7%) | 36 (62.1%) |
| AGE, MEAN (S.D.) | 59.2 (5.289) | 67.3 (5.448) |
| YEARS OF EDUCATION, MEAN (S.D.) | 15.2 (3.009) | |
| MEMORY | | |
| COMPOSITE SCORE, MEAN (S.D.) | 0.014 (0.925) | 0.108 (1.411) |
| FCSRT (SUM OF ALL FREE RECALLS), MEAN (S.D.) | 34.228 (5.159) | 33.017 (5.969) |
| MST (RECOGNITION MEMORY SCORE), MEAN (S.D.) | 0.792 (0.153) | 0.786 (0.183) |
| EXECUTIVE | | |
| COMPOSITE SCORE, MEAN (S.D.) | −0.038 (0.908) | −0.113 (2.475) |
| 2-MIN VERBAL LITERAL FLUENCY, MEAN (S.D.) | 24.660 (7.076) | 26.996 (7.312) |
| 2-MIN VERBAL CATEGORIAL FLUENCY, MEAN (S.D.) | 33.820 (7.032) | 33.724 (7.013) |
| DIGIT SPAN (INVERSE ORDER), MEAN (S.D.) | 6.614 (2.182) | 6.810 (2.290) |
| TMT (RT FOR PART B), MEAN (S.D.) | 68.673 (20.331) | 64.776 (20.817) |
| N-BACK (3-BACK VARIANT, D-PRIME), MEAN (S.D.) | 0.673 (0.145) | −0.115 (1.090) |
| ATTENTION | | |
| COMPOSITE SCORE, MEAN (S.D.) | 0.039 (0.981) | −0.112 (2.301) |
| DSST (2-MIN SCORE), MEAN (S.D.) | 72.560 (12.629) | 72.155 (11.309) |
| TMT (RT FOR PART A), MEAN (S.D.) | 31.703 (8.671) | 29.000 (8.615) |
| N-BACK (1-BACK VARIANT, D-PRIME), MEAN (S.D.) | 0.976 (0.041) | −0.112 (1.308) |
| D2 (GZ-F SCORE), MEAN (S.D.) | 401.730 (72.233) | 412.448 (61.843) |
| AB AND TAU/NEUROINFLAMMATION-PET IMAGING | | |
| TAU/NEUROINFLAMMATION BURDEN | | |
| NUMBER OF PARTICIPANTS | 64 | 40 |
| NUMBER OF FEMALES, *N* (%) | 42 (65.6%) | 25 (62.5%) |
| THK-PET IN BRAAK I/II ROIS, MEAN (S.D.) | 2.289 (0.247) | 2.307 (0.277) |
| B-AMYLOID BURDEN | | |
| NUMBER OF PARTICIPANTS | 90 | 57 |
| NUMBER OF FEMALES, N (%) | 68 (67.3%) | 36 (63.2%) |
| B-AMYLOID EARLY STAGE, MEAN (S.D.) | 0.855 (0.052) | −5.590 (8.794) |
| MRI | | |
| CORTICAL GRAY MATTER VOLUME ($MM^3$), MEAN (S.D.) | 458,647.230 (39,834.230) | |

Demographic information, cognitive scores, tau (THK-PET in Braak I/II ROIs) and β-amyloid burden (in early-stage deposition), and structural measures are presented for the entire sample at baseline and for 58 participants after 7-year follow-up. PET imaging (tau and β-amyloid) was only conducted at baseline; values at follow-up correspond to the subset of participants who underwent PET at baseline and were reassessed cognitively after 7 years. Mean (standard deviations) are provided

## NEUROPSYCHOLOGICAL ASSESSMENT

At the first visit, neuropsychological assessment was administered in two 1.5-h sessions and consisted of a battery of cognitive tests assessing three specific domains: memory, attention, and executive functions. The raw scores were converted to *z*-scores and three domain-specific composite scores were computed as the standardized sum of *z*-scores of the domain-specific scores, where higher values indicate better performance. As part of the memory assessment, we also considered the recognition

*Published in : GeroScience (2025)*
*DOI: 10.1007/s11357-025-01974-2*
*Status : Postprint (Author's version)*

memory score of the Mnemonic Similarity Task (MST; [78]), which evaluates the ability to visually recognize images of objects that were incidentally encoded. Previous published work on the COFITAGE database [19, 71], in line with the literature [67], showed that this MST score might be an early cognitive marker of memory decline. Analyses focused on the three composite scores and the MST recognition memory score. Seven years later, a similar follow-up neuropsychological assessment was administered and the same procedure was used to compute the three composite scores. For each score, a cognitive decline score was calculated as the baseline performance minus the follow-up performance, divided by the baseline performance, so that a negative score reflects a decline over the 7 years and a positive score reflects a cognitive gain (all the cognitive scores are detailed in **Table 1**).

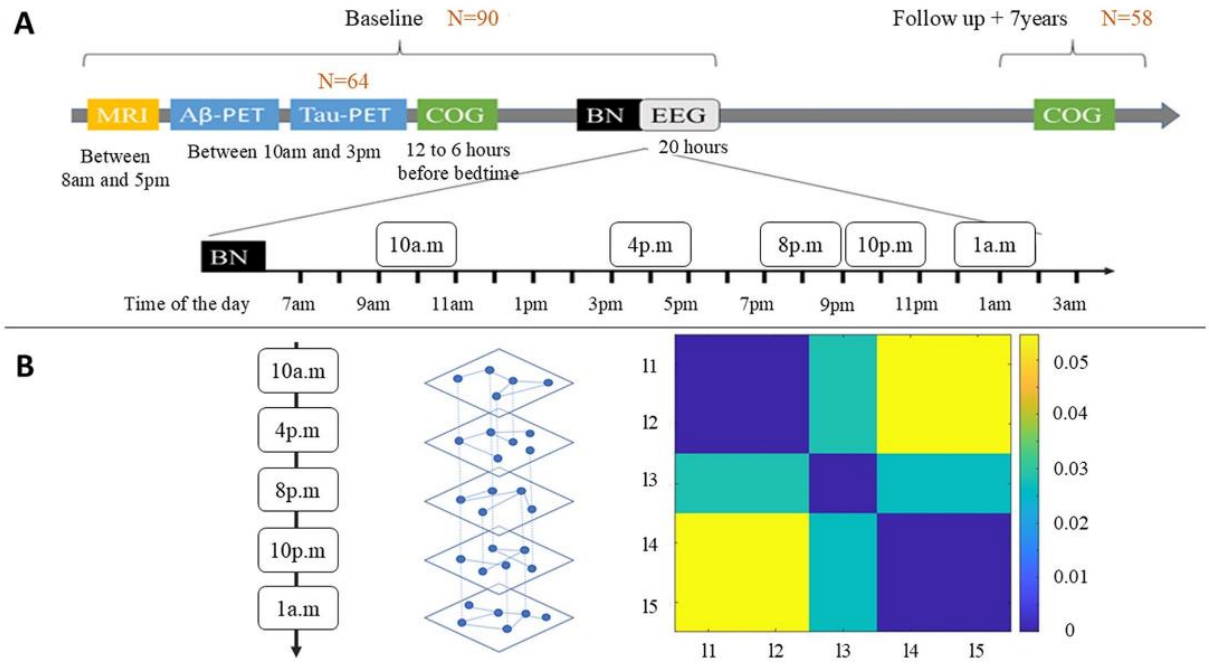


**Fig. 1** Experimental protocol and multilayer network analysis of diurnal rsFC dynamics. **A**) Experimental protocol, adapted from Van Egroo et al. [86]. COG cognitive assessment, BN baseline-night. **B**) Representation of the temporal multilayer network and Variation of Information (VI) matrix ($\omega = 0.5$ and $\gamma = 1.03$) at the group level. For each participant, we constructed two temporal multilayer networks (theta and gamma), composed of five functional layers of PLI matrices, featuring the 5 EEG sessions in their chronological order. In each layer, nodes were connected by edges only to their corresponding nodes in other layers in a consecutive or chronological order. VI matrix showed how community structure changes over layers at the group level and revealed 3 time periods in the daily organization of brain regions' communities at the group level

## SALIVARY MELATONIN ASSESSMENT

Salivary melatonin was measured by radioimmunoassay (Stockgrand Ltd, Guildford, UK). The detection limit of the assay for melatonin was 0.8 ± 0.2 pg/l using 500 µl volumes. To account for the fact that each participant's circadian phase is different, and that the course of the protocol might vary slightly between individuals, we considered the dim-light melatonin onset time (DLMO). DLMO was computed for each participant using the hockey-stick method, with the ascending level set to 2.3 pg/ml (Hockey-Stick software v1.5). Saliva samples were collected every hour in order to specify individuals'

*Published in : GeroScience (2025)*
*DOI: 10.1007/s11357-025-01974-2*
*Status : Postprint (Author's version)*

endogenous circadian rhythmicity during time awake by computing the phase between individuals' wake-up time and individuals' DLMO time (DLMO = phase 0°; 15° = 1 h), since we were interested in fluctuations over the course of the day.

## PET IMAGING

Amyloid-β PET and Tau/neuroinflammation-PET imaging were performed on an ECAT EXACT+ HR scanner (Siemens, Erlangen, Germany). β-Amyloid-PET imaging was performed with radiotracers [18F] Flutemetamol except for three subjects for which [18F]Florbetapir was used. Tau/neuroinflammation-PET imaging was performed with [18F]THK5351 for all subjects. For both β-amyloid and tau/neuroinflammation-PET imaging, a standardized uptake value ratio (SUVR) was calculated (**Table 1**). As β-amyloid-PET imaging was acquired using different radioligands, their SUVR values were converted into Centiloid units (in line with previous works of this cohort, see [86] and [62]. Volumes of interest were determined using the automated anatomical labeling atlas (AAL, [82]). β-Amyloid burden was averaged over composite masks covering neocortical regions reported to undergo the earliest aggregation sites for β-amyloid pathology (frontal medial cortex, fusiform gyrus, and temporal gyrus), while Tau/neuroinflammation burden was averaged over regions corresponding to Braak stages of early regional tau pathology (entorhinal cortex and hippocampus). The detailed PET imaging procedure was previously published in [62].

## ANATOMICAL DATA

Participants' T1-weighted MRI acquisition was performed on a 3Tesla MR scanner (MAGNETOM Prisma, Siemens) to assess brain gray matter integrity (**Table 1**). The following parameters were used: repetition time (TR) = 18.7 ms; flip angle (FA) = 20 degrees; 3D multiecho fast low angle shot (FLASH) sequence (TR/ FA) = 136,166; voxel size = 1 $mm^3$ isotropic; acquisition time of all structural sequences = 19 min (see Van Egroo et al. [86] for detailed parameters). The FreeSurfer [31] software was used to generate cortical surfaces and automatically segment cortical structures from each participant's T1-weighted anatomical MRI, to account for individual brain anatomy during source reconstruction.

## EEG RECORDING AND ANALYSES

### DATA ACQUISITION

For each participant, 2 min of resting-state EEG (sampling rate = 1450 Hz, bandpass filter = 0.1–500 Hz) was recorded five times throughout the wake-extension protocol (for example at 10:00 a.m., 4:00 p.m., 8:00 p.m., 10:00 p.m., and 1:00 a.m. for a participant waking up at 7:00 am) with a 60-channel EEG system (Eximia, Nexstim, Helsinki, Finland) covering the whole scalp. Participants were instructed to relax and avoid blinking while staring at a black dot.

### PRE-PROCESSING

Artifact and channel rejection (on continuous data), filtering (0.5–40 Hz bandpass, on unepoched data), re-referencing (i.e., using the algebraic average of the left TP9 and right TP10 mastoid electrodes), and source estimation were performed using Brainstorm [79]. Physiological artifacts

*Published in : GeroScience (2025)*
*DOI: 10.1007/s11357-025-01974-2*
*Status : Postprint (Author's version)*

(blinks, saccades) were identified and manually removed through Independent Component Analyses (ICA) using the Infomax algorithm (EEGLAB, runica.m). The Independent Component Analyses approach consists of removing artifacts from the recording without removing the affected data portions, by identifying spatial components that are independent in time and uncorrelated with each other [79]. Source estimates were aligned to a standard space (i.e., ICBM152 template) using Brainstorm's automated spatial registration pipeline with individual FreeSurfer surfaces. This ensured accurate cortical surface alignment across participants.

### SOURCES RECONSTRUCTION

FreeSurfer [31] segmentation of individuals' T1-weighted anatomical MRI was used to constrain the source reconstruction and account for individual anatomy. The EEG forward model was obtained from a symmetric boundary element method (BEM model,OpenMEEG, [35]), fitted to the spatial positions of each electrode. A cortically constrained sLORETA procedure [65] was applied to estimate the cortical origin of scalp EEG signals. The estimated sources were then projected onto the ICBM152 standard space for comparisons between groups and individuals, while accounting for differences in native anatomy.

### PLI MATRICES CONSTRUCTION

The individual alpha-peak frequency (IAF) observed at occipital sites was used to estimate the range of each frequency band. Based on previous works [38, 81], the following five frequency bands were considered: delta (IAF – [6–8] Hz), theta (IAF – [2–6] Hz), alpha (IAF + [−2 to 2] Hz), beta (IAF + [2–14] Hz), and gamma1 (IAF + [15–30] Hz). Phase-lag index (weighted PLI analyses; [76]) was used to assess the phase synchrony between 68 regions of interest (ROI, 68 ROIs as 34 contralateral homologous ROIs) defined by using the Desikan-Kiliany brain atlas [23]. For each participant, we obtained 5 × 5 PLI matrices of 68 × 68 ROIs couplings, with one matrix per frequency band for each of the five EEG recording sessions. PLI analyses estimate the variability of phase differences between two regions over time. Similar phase difference across time is indicated by a PLI value close to 1 (i.e., high synchrony between regions), while large variability in the phase difference is indicated by a PLI value close to 0. The PLI measure has been shown to be less sensitive to the influence of common sources and amplitude effects relative to phase-locking value, as it disregards zero phase lag that could reflect volume conduction artifacts [76]. The following analyses are focused only on the theta and gamma frequency bands, as our previous study showed their specific implication in diurnal brain dynamics in healthy aging [9]..

## MULTILAYER NETWORK ANALYSES

### TEMPORAL MULTILAYER NETWORK

Using BRAPH 2 software ([16, 57], https://github.com/braph-software/BRAPH-2/releases/tag/2.0.0.a4) and following a procedure detailed in CanalGarcia et al. [13], we created two temporal multilayer networks for each participant, one for the theta and another one for the gamma frequency band. Each temporal multilayer network is composed of five "functional" layers of 68 × 68 PLI matrices, always featuring the five EEG sessions in their chronological order (Pipeline Ordered-Multiplex Connectivity

*Published in : GeroScience (2025)*
*DOI: 10.1007/s11357-025-01974-2*
*Status : Postprint (Author's version)*

Analysis using Weighted Undirected graphs). In each layer, nodes were connected by edges only to their corresponding nodes in other layers in a consecutive or chronological order (**Fig. 1**B).

## MULTILAYER COMMUNITY STRUCTURE

A community detection approach [60] was used to cluster groups of nodes that are more highly connected to one another than to nodes outside their communities across the five layers, by computing the generalized multilayer modularity $Q$ as follows: $Q = \frac{1}{2\mu} \sum_{ijsr} [(A_{ijs} - \gamma P_{ijs})\delta_{sr} + \delta_{ij}\omega_{jsr}]\delta(g_{is}, g_{jr})$, where $\mu$ is the total weights of the edges, $A_{ijs}$ is the adjacency matrix between nodes $i$ and $j$ at layer $s$, $\gamma$ is the resolution parameter, which sets the weights of intralayer connections at layer $s$, $P_{ijs}$ is the associated null matrix (i.e., edges randomization of each layer while maintaining node strength) at layer $s$, $\delta_{sr} = 1$ if $s = r$ and 0 otherwise, $\omega$ is the temporal resolution parameter which determines the weights of the inter-layer edges, $\delta_{ij} = 1$ if $i = j$ and 0 otherwise, $g_{is}$ and $g_{jr}$ are the community allegiances of node $i$ at layer $s$ and node $j$ and layer $r$ respectively, and $\delta(g_{is}, g_{jr}) = 1$ if the community allegiances $g_{is}$ and $g_{jr}$ of nodes $i$ and $j$ at layer $s$ and $r$ are the same and 0 otherwise. Low $\gamma$ values produced fewer but larger communities, while high values resulted in more but smaller communities. Small $\omega$ values emphasized unique community structures per layer, while larger values highlighted shared community structures across layers, representing potential community structures that do not change over time [13, 68]. We chose intermediate values, such as $\omega$ = 0.5 and $\gamma$ = 1.03, following previous work comparing $\omega$ and $\gamma$ values (Matter et al., 2015 [68],), so as to maximize the variability of the flexibility coefficient across brain regions. At the group level, we obtained 3 community structures across the five temporal layers, in both theta and gamma, which have been used to initialize individuals' analyses. Finally, to enhance the robustness of the communities found in each layer, we performed 100 iterations of the multilayer modularity optimization algorithm for each participant, with each iteration initialized using the group-level community structure. This iterative approach ensured that the final community assignments were stable and not dependent on a single initialization. Variation of Information (VI) matrices averaged across all participants were plotted to visualize how the community structure evolve over layers (i.e., over time) at group level (**Fig. 1**B). Each cell in the matrix represents the VI value between the community structures of the corresponding layers. Low VI values indicate that community structures are similar over layers reflecting a stable functional connectivity over time, whereas high VI values indicate that community structures are different over layers suggesting variability of functional connectivity over time. VI matrix revealed 3 time periods in the diurnal organization of brain regions communities: (1) stable organization of brain regions communities between the first and the second layers and between the fourth and the fifth layers, (2) major reorganization of brain regions communities between the first two layers and the last two layers, (3) moderate changes in the organization of brain regions communities between the third layer and the other layers suggesting that the third layer might be a transition period.

## MODULE ALLEGIANCE MATRIX AND DYNAMIC NETWORK MEASURES

To further investigate the temporal dynamics of brain network modularity, we computed and plotted the module allegiance matrix for each participant, which measures the probability that a pair of nodes (two brain regions) are assigned to the same community over time and repetitions [54] (**Fig. 2**, left). The matrix $M$ consists of 68 × 68 pair of nodes and can be written as $M_{ij} = \frac{1}{OT} \sum_{0=1}^{O} \sum_{t=1}^{T} a_{i,j}^{k,o}$, where $O$ is

*Published in : GeroScience (2025)*
*DOI: 10.1007/s11357-025-01974-2*
*Status : Postprint (Author's version)*

the number of iterations of the multilayer community detection algorithm and $T$ is the number of layers. For each optimization $O$ and layers $T$, if they are in the same community network, the value of module allegiance is 1 (the values on the main diagonal of the matrix are all 1); otherwise, it is 0.

To quantify the dynamic role of a region within and between brain networks, we calculated dynamic network recruitment and the dynamic network integration coefficient based on the module allegiance matrix [7, 54]. For this purpose, six resting-state networks were predefined based on Uddin et al. [84] classification: Central Executive Network (CEN), Salience Network (SN), Default Mode Network (DMN), Dorsal Attention Network (DAN), Visual System (VS), and Sensorimotor Network (SMN). Brain regions were assigned to these networks according to this classification, and module allegiance was subsequently calculated as a result of the community detection algorithm. Dynamic recruitment coefficient was defined as the probability that a region is assigned to the same network community as other regions from the same network over layers and repetitions. For node $i$ in the community network $S$, the dynamic recruitment can be computed as follows: $R_i^S = \frac{1}{n_s} \sum_{j \in S} P_{ij}$, where $n_s$ is the number of nodes in the network $S$. $P_{ij}$ represents the number of times that nodes $i$ and $j$ are assigned to the same community. Dynamic integration was defined as the probability that a region is assigned to the same network community as regions from other networks across layers and repetitions. For node $i$ in the community network $S$, the dynamic recruitment can be computed as follows: $I_i^S = \frac{1}{N - n_s} \sum_{j \notin S} P_{ij}$, where $N$ is the total number of brain regions. For each participant, both recruitment and integration coefficients obtained for each brain regions were averaged by networks to quantify brain networks' dynamic recruitment and integration over time (**Fig. 2**, right). Although the dynamic recruitment and integration coefficients were computed based on all 68 regions from the six predefined networks, we focused the analyses and visualizations on the three core cognitive networks (DMN, SN, and CEN) due to their critical roles in cognitive functioning and aging-related changes. This selection aligns with prior literature highlighting these networks as central to higher-order cognitive processes and their sensitivity to aging and neurodegeneration [48, 55]. Module allegiance matrix enables to visualize brain networks' dynamics [54], as the diagonal of the matrix represents the dynamic recruitment and the off-diagonal represents the dynamic integration [7] (**Fig. 2**).

*Published in : GeroScience (2025)*
*DOI: 10.1007/s11357-025-01974-2*
*Status : Postprint (Author's version)*

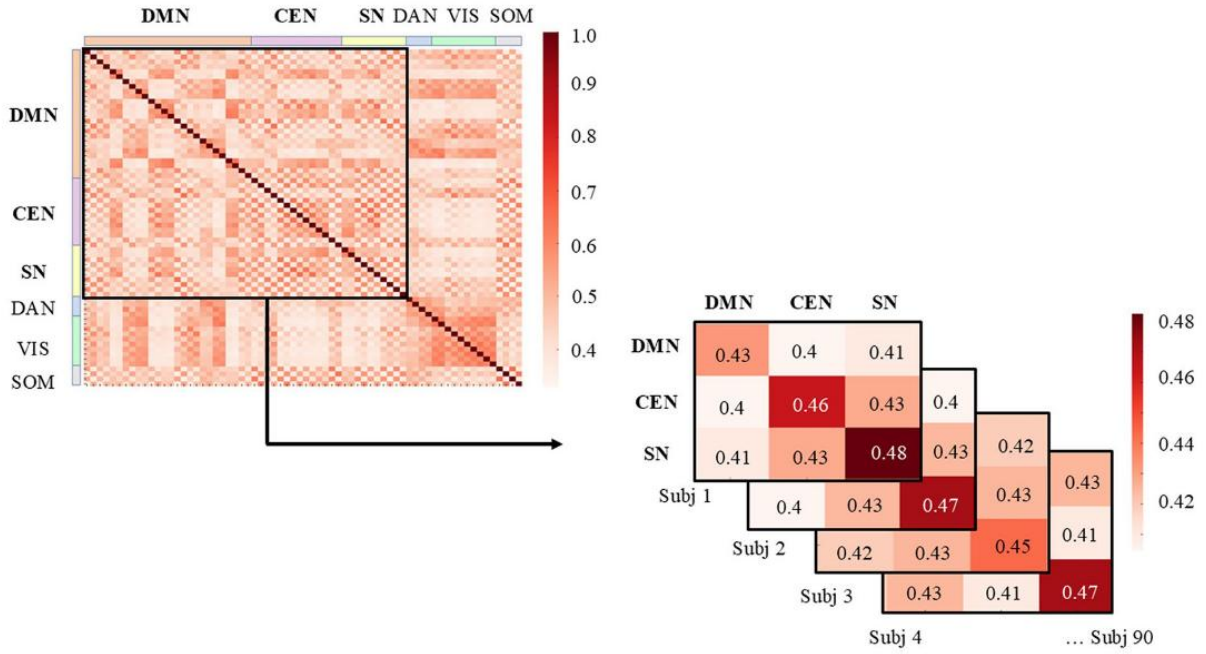


**Fig. 2** Multilayer network analysis of diurnal rsFC dynamics. Module allegiance matrix of brain regions (left), averaged by networks (right), both for each participant. The diagonal of the matrices represents the dynamic recruitment and the off-diagonal represents the dynamic integration

### STATISTICAL ANALYSES

To statistically assess the differences between the DMN, SN, and CEN networks' recruitment and integration dynamic measures over time in theta and gamma bands, 3 (*networks*: DMN, CEN, SN) × 2 (*dynamic measures*: integration, recruitment) × 2 (*frequency bands*: theta, gamma) repeated-measures ANOVAs with subjects as a random factor were applied using JASP (https://jasp-stats.org/; version 0.18.1). The Greenhouse-Geisser epsilon correction was applied to the factor *networks* where Mauchly's test indicated a violation of the sphericity assumption. Original degrees of freedom and corrected $p$-values are reported. Finally, regressions aimed at determining the association of dynamic recruitment and integration measures of each network in theta and gamma frequency bands, with cognitive performances scores at baseline, cognitive decline scores (the three domain-specific composite scores and the recognition memory score of the MST) and β-amyloid rates and tau/neuroinflammation burden rates (the latter only available for 64 participants). Results were FDR-corrected for multiple comparisons [8], with a significance threshold of $q < 0.05$ applied separately to each set of comparisons (2 comparisons for ANOVA, and 3 to 4 comparisons for each regression analysis set). Participants' age, sex, and mean gray matter volume and individuals' wake-up/DLMO phase value were included as covariates in the analyses.

## Results

We analyzed data from 90 healthy late middle-aged adults (50–69 years old) from the COFITAGE (COgnitive FITness in AGEing) database [see Materials and Methods and [9, 18, 19, 62, 71, 85, 86]],

*Published in : GeroScience (2025)*
*DOI: 10.1007/s11357-025-01974-2*
*Status : Postprint (Author's version)*

who underwent five resting-state EEG recordings over the course of a single day (10 a.m., 4 p.m., 8 p.m., 10 p.m., and 1 a.m.). rsFC was measured using the Phase Lag Index (PLI), which quantifies synchronization between brain regions, in theta (4–8 Hz) and gamma (30–100 Hz) bands. To capture rsFC dynamics in theta and gamma bands, we constructed two time-varying multilayer networks, where each PLI matrix represents a layer reflecting the rsFC pattern at a given time, allowing us to measure dynamic recruitment and integration. Higher rsFC fluctuations corresponded to lower recruitment and integration scores, indicating reduced network stability. In addition to EEG, cognitive assessments at baseline and after 7 years, along with tau and β-amyloid markers, were collected to examine the associations between rsFC, cognitive trajectories, and pathological aging processes.

## NETWORKS' DIURNAL RECRUITMENT AND INTEGRATION DYNAMICS ARE SIMILAR IN THETA AND GAMMA

We performed a repeated-measures ANOVA (networks × dynamic measures × frequencies) to determine how the regions of our 3 brain networks of interest were recruited and integrated over the day in both theta and gamma frequency bands. The analysis first yielded a significant effect of dynamic measure ($F$ (1,170) = 347.489, $p$ < 0.001, $\eta p^2$ = 0.803), with higher dynamic recruitment compared to the integration of brain networks' regions over time (**Fig. 3**). The interaction between network and dynamic measure ($F$ (2,170) = 245.431, $p$ < 0.001, $\eta p^2$ = 0.743) revealed that the recruitment of the SN (M = 0.464, SE = 0.006) is significantly higher than the recruitment of the CEN (M = 0.450, SE = 0.005), which is also significantly higher than the recruitment of the DMN (M = 0.415, SE = 0.004) (**Fig. 3**B). Moreover, dynamic integration was significantly higher for DMN brain regions (M = 0.405, SE = 0.004) than for both the SN (M = 0.402, SE = 0.004) and the CEN brain regions (M = 0.399, SE = 0.004) (**Fig. 3**A). No interaction with the frequency band was found, indicating that these patterns of results did not significantly differ between theta and gamma bands.

*Published in : GeroScience (2025)*
*DOI: 10.1007/s11357-025-01974-2*
*Status : Postprint (Author's version)*

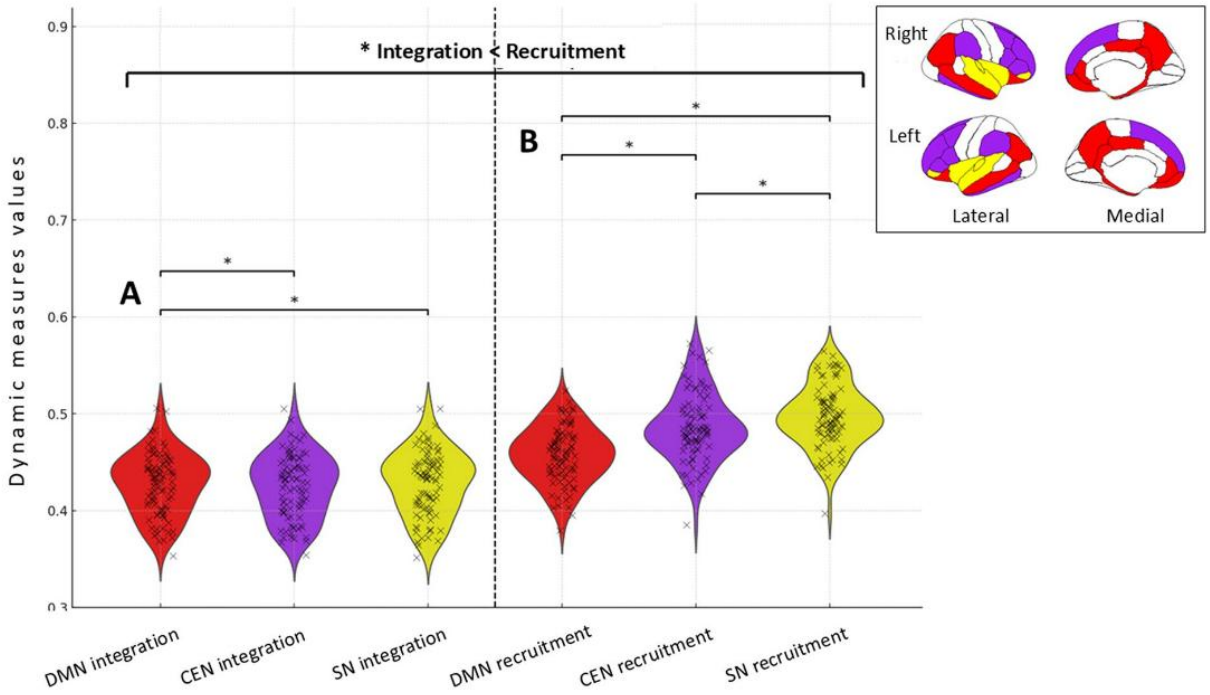


**Fig. 3** Dynamic recruitment is higher than integration across DMN, SN, and CEN in theta and gamma bands. Violin plots illustrate higher dynamic recruitment (right) than integration (left) across DMN (red), SN (yellow), and CEN (purple) over time in the theta and gamma bands. **A**) Integration: DMN (M = 0.405, SE = 0.004) was significantly higher than both SN (M = 0.402, SE = 0.004) and CEN (M = 0.399, SE = 0.004). **B**) Recruitment: SN (M = 0.464, SE = 0.006) was significantly higher than CEN (M = 0.450, SE = 0.005), which was in turn higher than DMN (M = 0.415, SE = 0.004). (B) Integration: DMN (M = 0.405, SE = 0.004) was significantly higher than both SN (M = 0.402, SE = 0.004) and CEN (M = 0.399, SE = 0.004). Brain maps (top right) highlight the corresponding regions in each network

## THETA AND GAMMA DIURNAL DYNAMIC NETWORK MEASURES ARE DIFFERENTLY ASSOCIATED WITH COGNITIVE PERFORMANCE

To test whether diurnal dynamic measures (integration and recruitment) could explain part of individual differences in cognitive performance among older individuals, we assessed their associations with cognitive performance at baseline and with cognitive decline after a 7-year follow-up. Specifically, we assessed how dynamic recruitment and integration of the SN, CEN, and DMN in both theta and gamma bands related to three domain-specific composite scores, the recognition memory score (MST), and their corresponding cognitive decline scores. For all the results below, no effect of age, sex, and mean gray matter volume or individuals' wake-up/DLMO phase value was found, indicating that these factors did not significantly contribute to the observed associations. The correlation matrix in **Fig. 4**C provides Pearson's $R$-values of the associations assessed through regression analyses.

*Published in : GeroScience (2025)*
*DOI: 10.1007/s11357-025-01974-2*
*Status : Postprint (Author's version)*

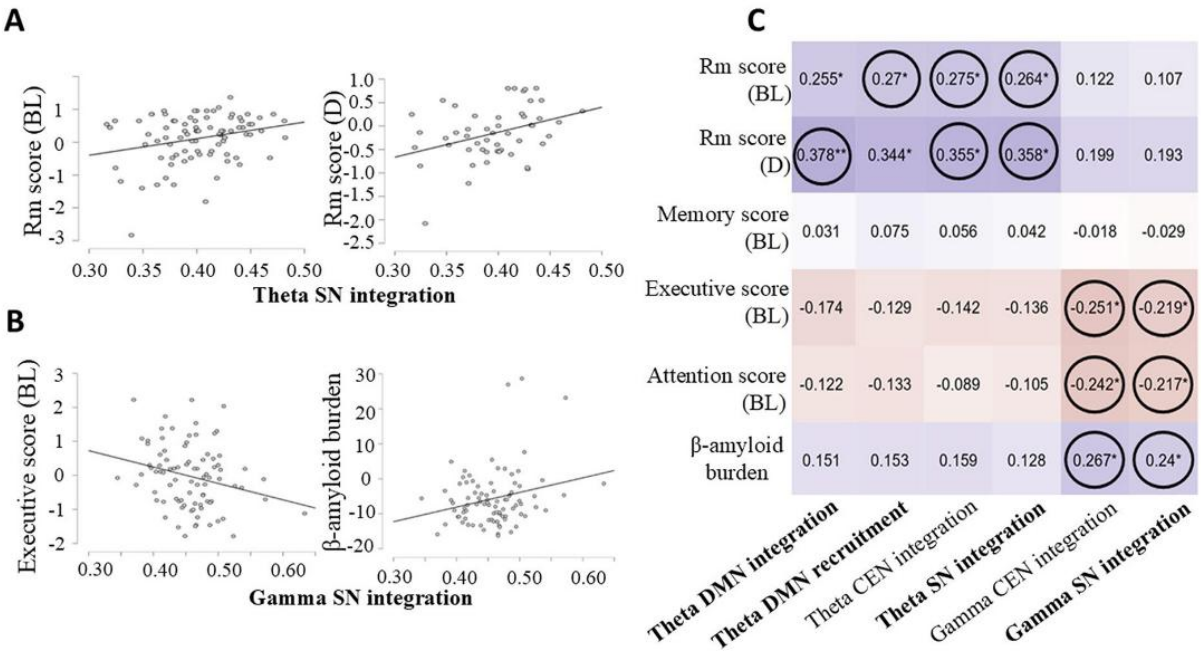


**Fig. 4** Distinct associations between theta and gamma SN integration, cognitive performance, and β-amyloid burden. Scatter plots illustrate key associations between SN integration and cognitive performance. **A**) In the theta band, higher SN integration is associated with higher memory performance at baseline (left) and with lower longitudinal memory decline (right). **B**) In contrast, in the gamma band, higher SN integration is associated with lower executive performance at baseline (left) and higher β-amyloid burden (right). **C**) Correlation matrix shows $R$-values of Pearson's correlations (*$p$ <.05, **$p$ <.01; positive correlation: blue, negative correlation: red); black circles indicate results that survived when FDR-corrected for multiple comparisons [8]. BL = baseline cognitive performance; D = decline in performance between baseline and 7-year follow-up

## POSITIVE ASSOCIATION OF DIURNAL DYNAMIC DMN RECRUITMENT AND DIURNAL DYNAMIC SN AND CEN INTEGRATION IN THETA BAND WITH MEMORY PERFORMANCE AT BASELINE

Regression analyses showed that DMN diurnal dynamic recruitment and SN and CEN diurnal dynamic integration coefficients in the theta band were positively correlated with the recognition memory score of the MST at baseline (DMN: $\beta$ = 5.506, $t$ = 2.580, $p$ = 0.012, FDR-corrected $p$ = 0.0325; SN: $\beta$ = 5.049, $t$ = 2.505, $p$ = 0.014, FDR-corrected $p$ = 0.04; CEN: $\beta$ = 5.442, $t$ = 2.621, $p$ = 0.010, FDR-corrected $p$ = 0.04). These results indicate that higher dynamic recruitment of DMN and higher dynamic integration of SN and CEN brain regions across the day in the theta band is associated with higher memory performance at baseline (**Fig. 4**A left).

## NEGATIVE ASSOCIATION OF SN AND CEN DIURNAL DYNAMIC INTEGRATION IN GAMMA BAND WITH EXECUTIVE AND ATTENTION PERFORMANCE AT BASELINE

Regression analyses showed that SN and CEN diurnal dynamic integration coefficients in the gamma band were negatively correlated with the executive composite score (SN: $\beta$ = −4.818, $t$ = −2.376, $p$ = 0.020, FDR-corrected $p$ = 0.04; CEN: $\beta$ = −5.275, $t$ = −2.678, $p$ = 0.009, FDR-corrected $p$ = 0.018) and the attention composite score (SN: $\beta$ = −5.627, $t$ = −2.609, $p$ = 0.011, FDR-corrected $p$ = 0.04; CEN: $\beta$ =

*Published in : GeroScience (2025)*
*DOI: 10.1007/s11357-025-01974-2*
*Status : Postprint (Author's version)*

−5.993, $t$ = −2.858, $p$ = 0.005, FDR-corrected $p$ = 0.018) both at baseline. In other words, higher dynamic integration of SN and CEN brain regions across the day in the gamma band is associated with lower executive and attention performance at baseline (**Fig. 4**B left).

### POSITIVE ASSOCIATION OF DIURNAL DYNAMIC DMN, SN, AND CEN INTEGRATION IN THETA BAND WITH LONGITUDINAL MEMORY DECLINE

Regression analyses showed that DMN, SN, and CEN diurnal dynamic integration coefficients in the theta band were positively correlated with the recognition memory score of the MST decline score (DMN: $\beta$ = 5.682, $t$ = 2.825, $p$ = 0.007, $p$ = 0.011, FDR-corrected $p$ = 0.028; SN: $\beta$ = 5.328, $t$ = 2.657, $p$ = 0.011, FDR-corrected $p$ = 0.044; CEN: $\beta$ = 5.334, $t$ = 2.633, $p$ = 0.011, FDR-corrected $p$ = 0.012). That is, higher dynamic integration of DMN, SN, and CEN brain regions across the day in the theta band is associated with a lower memory decline after 7-year follow-up (**Fig. 4**A right).

### POSITIVE ASSOCIATION BETWEEN SN AND CEN DIURNAL DYNAMIC INTEGRATION IN GAMMA BAND AND EARLY B-AMYLOID BURDEN

Results showed that SN and CEN diurnal dynamic integration coefficients in the gamma band were positively correlated with β-amyloid burden rate (SN: $\beta$ = 51.179, $t$ = 2.493, $p$ = 0.015, FDR-corrected $p$ = 0.023; CEN: $\beta$ = 54.585, $t$ = 2.744, $p$ = 0.007, FDR-corrected $p$ = 0.009). Higher dynamic integration of SN and CEN brain regions across the day in the gamma band is associated with a higher β-amyloid burden (**Fig. 4**B right).

## Discussion

Brain region's rsFC variability is increasingly considered to be predictive of cognitive performance in aging [20, 33, 38–40], [45, 83], reflecting the dynamic reorganization of brain regions. Furthermore, the switching rates between different network communities have been associated with cognitive performance [66]. Our main goal was therefore to characterize brain network's rsFC diurnal dynamics in healthy cognitive aging. Using a multilayer network approach, we investigated theta and gamma rsFC variability across five recordings over 20 h of continuous (mainly daytime) waking, in late middle-aged healthy participants (50–69 years). Our results shed new light on (a) how brain regions are integrated and recruited across the day in relation to their resting-state network and network communities, (b) the associations of so-called diurnal dynamic networks' recruitment and integration with cognitive performance, and (c) their associations with cognitive decline and with biological markers of Alzheimer's disease (AD).

### THETA AND GAMMA DIURNAL DYNAMIC REORGANIZATION OF DMN, SN, AND CEN

We first showed that DMN, SN, and CEN brain regions were more often recruited with regions belonging to the same network community than other communities across the day, both in theta and gamma band. In other words, over the day, rsFC of brain regions tended to remain within the same

*Published in : GeroScience (2025)*
*DOI: 10.1007/s11357-025-01974-2*
*Status : Postprint (Author's version)*

community rather than to switch between communities. This finding suggests that the functional specialization of brain networks is preserved over the course of the day, while the integration between different networks fluctuates to a greater extent. This interpretation appears to contrast with the findings of a previous fMRI study that compared network dynamics between morning and evening sessions in young adults [27]. Their results showed greater integration than recruitment in the evening compared to the morning, which was interpreted as a reflection of functional dedifferentiation occurring over the day. However, their conclusions were based on a comparison of rsFC at only two discrete time points and did not capture the continuous evolution of functional network organization across the day. Our study provides additional information about extended diurnal dynamics of rsFC brain networks as our multilayer model accounts for five different times of the day ordered in a 20-h time-frame. By using a finer-grained temporal resolution through the incorporation of intermediate recordings between morning and evening, we reveal that brain networks maintain a stable recruitment pattern throughout the day, preserving their functional specialization, while integration fluctuates more dynamically. These additional time points offer new insights into the temporal evolution of rsFC and highlight the importance of considering fine-grained temporal resolution when studying brain network dynamics.

Diurnal dynamic recruitment of brain regions over time indicated that rsFC reorganization, or rsFC variability, over the day was higher within the SN than the CEN and then the DMN. Previous studies showed that the SN is involved in the regulation of arousal, as rsFC alterations within the SN were reported in individuals with sleep disturbance [43, 52]. Thus, high rsFC reorganization within the SN might reflect the progressive build-up of sleep need during prolonged wakefulness. Conversely, lower rsFC within the DMN during the day has been associated with lower maintenance of wakefulness and might also reflect the build-up of sleep pressure [26]. Lower reorganization of DMN brain regions' rsFC might indicate its lower implication as the day progresses. Brain regions of the CEN exhibit an intermediate rate of rsFC reorganization across the day, in line with previous studies characterizing the CEN as the most stable resting-state network across the day [10]. Finally, our results showed that diurnal dynamic integration of brain regions over time was higher for the DMN than for the SN and CEN, indicating that over the day, DMN regions exhibited greater reorganization with other network communities compared to SN and CEN regions. This result is consistent with previous studies in healthy young adults, showing that higher integration of DMN regions with other networks over the day is associated with deliberate mind-wandering and introspective processes [27, 34]. The DMN, SN, and CEN play a crucial role in cognitive aging due to their involvement in key cognitive processes such as attention, memory, and executive functions [55, 56]. The SN regulates the balance between DMN activity, which supports internally directed cognition, and CEN activity, which is involved in goal-directed tasks such as working memory and attentional control [17]. Aging has been associated with changes in the functional organization of these networks, including increased integration among them [63], which has been interpreted as a compensatory mechanism to counteract cognitive decline. Specifically, studies have shown that altered SN-DMN interactions are observed in individuals with mild cognitive impairment [15], and that reorganization of these large-scale networks is a key marker of cognitive aging [48]. Taken together, our results suggest that the diurnal dynamic recruitment and integration of the DMN, SN, and CEN networks are critical for maintaining cognitive function in aging.

*Published in : GeroScience (2025)*
*DOI: 10.1007/s11357-025-01974-2*
*Status : Postprint (Author's version)*

## HIGH DIURNAL THETA SN, CEN, AND DMN DYNAMICS ARE ASSOCIATED WITH BETTER MEMORY PERFORMANCE AT BASELINE AND LOWER LONGITUDINAL MEMORY DECLINE

Our results reveal that higher diurnal dynamic integration of both SN and CEN brain regions, and higher diurnal dynamic recruitment of DMN brain regions, all in the theta band, were associated with higher memory performance at baseline. This concerns the recognition memory score of the MST, which has been shown to be a sensitive measure to detect subtle general cognitive decline in aging [19, 67, 71].

Results concerning SN and CEN are in line with previous studies, showing increased integration of brain networks during aging, associated with similar cognitive performance as younger adults [25, 42, 77]. These positive associations with cognitive performance could reflect a compensatory response to reduced network specialization in older adults [22, 37, 44, 53, 74, 88]. However, our results might indicate that this compensation is most effective when brain network integration remains stable throughout the day. The increased integration of SN and CEN may therefore reflect an adaptive reorganization of large-scale network dynamics, helping to counteract the decline in network segregation commonly observed in aging [22, 37, 44, 53, 74, 88]. In this context, our findings suggest that, rather than transient increases in rsFC, maintaining stable integration of SN and CEN regions in the theta band throughout the day is essential for sustaining memory performance. Unlike SN and CEN regions, DMN regions appear to maintain stable within-network rsFC throughout the day in the theta band, which is also associated with preserved memory performance at baseline. This finding is in line with a study showing that, while SN and CEN exhibit early functional changes and increased inter-network connectivity in normal cognitive aging, the DMN appears to maintain more sustained within-network functional connectivity [64]. As the largest brain network, the DMN consists of key hub regions involved in numerous cognitive processes, including memory [29]. Aging induces important reorganization of the rsFC between these hub regions to compensate for the loss of efficiency of these regions to maintain cognitive performance [2, 29]. Altogether, our results suggest that, in healthy cognitive aging, diurnal dynamic integration of SN and CEN regions might reflect a beneficial ability of brain network to reorganize across the day with other networks to maintain cognitive performance, whereas DMN brain regions remain functionally consistent across the day.

Furthermore, higher diurnal dynamic integration of SN, CEN, and DMN regions, in the theta band, was associated with lower memory decline after a 7-year follow-up. These findings refine our understanding of the adaptive mechanisms that support cognitive preservation in aging, by emphasizing the diurnal temporal dynamics of this compensatory process. Rather than a simple increase in inter-network connectivity, the ability to maintain stable rsFC patterns across the day appears to be a critical determinant of cognitive trajectories in aging. Specifically, stable inter-network rsFC throughout the day, particularly in the theta band, appears to be beneficial for memory in older adults, whereas fluctuations in internetwork connectivity may indicate a failure to sustain alternative compensatory networks, as it is associated with long-term memory decline. These findings suggest that cognitive benefits depend on efficient network communication, not just broader engagement [11, 70]. A stable rsFC throughout the day, particularly in the theta band, may thus reflect optimal network efficiency and be associated with better memory preservation in aging.

*Published in : GeroScience (2025)*
*DOI: 10.1007/s11357-025-01974-2*
*Status : Postprint (Author's version)*

Finally, our results highlight the central role of theta-band rsFC dynamics in memory and cognitive aging. Previous research has shown that aging is associated with an increase in slow rhythms activity, including theta, which reflects a general slowing of brain activity and has been linked to cognitive decline [41, 49]. Notably, theta-band rsFC has been identified as a key predictor of cognitive decline, including the progression from subjective cognitive complaints to mild cognitive impairment (MCI), and from MCI to Alzheimer's disease [3]. Theta band has long been associated with memory processes and large-scale network coordination [28], and enhanced theta rsFC has been linked to preserved memory performance in aging [30]. While no significant differences were observed across frequency bands in our study, the associations between diurnal rsFC dynamics and memory performance were exclusively linked to theta-band phase synchrony. This suggests that, within the theta frequency range, diurnal dynamic integration is associated with healthy cognitive trajectories in aging, regardless of the specific network involved.

## HIGH DIURNAL GAMMA SN AND CEN DYNAMIC INTEGRATION ARE ASSOCIATED WITH LOW EXECUTIVE AND ATTENTIONAL PERFORMANCE AT BASELINE

In contrast, higher diurnal dynamic integration of SN and CEN regions in gamma band, reflecting greater stability of rsFC across the day, was associated with lower executive and attentional performance. Conversely, greater fluctuations in gamma rsFC were associated with better executive and attentional functioning, suggesting that flexibility, rather than stability, in gamma band supports cognitive efficiency. These findings align with previous studies indicating that excessive integration of SN and CEN in aging, when accompanied by reduced performance, may reflect maladaptive network reorganization rather than a compensatory mechanism [63]. Moreover, a recent study reported that while localized gamma synchrony facilitates cognitive function, widespread gamma synchrony—akin to excessive connectivity stability—is associated with lower cognitive performance, particularly in tasks requiring high cognitive effort [4]. This pattern is consistent with the neural dedifferentiation hypothesis which suggests that aging leads to a loss of functional specialization [53]. However, a rigid gamma connectivity pattern appears detrimental to cognition. According to the Scaffolding Theory of Aging and Cognition (STAC, [70]), cognitive aging benefits from the adaptive engagement of alternative networks, highlighting the importance of gamma-band flexibility throughout the day.

This interpretation is supported by research showing that gamma oscillations play a key role in attentional control, cognitive flexibility, and information integration [50, 59]. In aging, a high degree of flexibility in gamma connectivity may reflect an ability to dynamically allocate cognitive resources, while excessive stability in gamma synchrony may indicate reduced adaptability and impaired executive efficiency. However, unlike the theta band, gamma dynamics were not associated with long-term cognitive trajectories. While gamma fluctuations may enhance momentary executive function, they do not necessarily predict preserved cognition over time. This absence of a long-term effect raises the possibility that gamma connectivity reflects a state of hyperexcitability that could be neurotoxic in the long run [24]. While some level of gamma flexibility appears beneficial, excessive fluctuations or persistent instability could disrupt efficient network coordination, potentially contributing to cognitive decline.

*Published in : GeroScience (2025)*
*DOI: 10.1007/s11357-025-01974-2*
*Status : Postprint (Author's version)*

## HIGH DIURNAL GAMMA SN AND CEN DYNAMIC INTEGRATION ARE ASSOCIATED WITH HIGH EARLY B-AMYLOID BURDEN RATE

In the gamma band only, we observed that higher diurnal dynamic integration of SN and CEN regions was associated with higher early β-amyloid burden. This result can be linked to recent findings showing increased widespread gamma synchrony in AD patients [5], reinforcing the idea that rsFC stability in the gamma band may be linked to early neuropathological processes. Considerable evidence suggests amyloid deposition precedes a decline in cognition and may be the initiator of a cascade of events that indirectly leads to cognitive decline [72]. Our results further refine this perspective by revealing that participants with greater rsFC stability in the gamma band throughout the day exhibited higher levels of early β-amyloid deposition, whereas those with greater fluctuations in gamma connectivity had lower β-amyloid burden. This finding suggests that a lack of flexibility in gamma connectivity may be an early biomarker of pathological changes in the brain. This is consistent with previous research indicating that the presence of β-amyloid proteins in their early deposition sites might disrupt the functional connectivity between large-scale networks, in particular the inter-connectivity of SN with other regions before the spread of the pathology that occurs later [36].

This aligns with neurostimulation studies showing that increased gamma-band flexibility can promote amyloid clearance [61]. Future research should clarify whether rigid gamma connectivity serves as an early indicator of β-amyloid pathology, either as a marker of emerging deposition or as a downstream effect of amyloid-related disruptions. While β-amyloid accumulation has been predominantly linked to the DMN [69], our findings highlight the role of diurnal SN–CEN integration in the gamma band, suggesting that amyloid-related processes may extend beyond the DMN.

## LIMITATIONS AND PERSPECTIVES

Our findings have some limitations. First, our results were obtained from healthy middle-aged to older participants whose global cognitive performance is in the upper average range, and none of them exhibited significant cognitive decline during the follow-up period. Therefore, the present results could differ in individuals aged 70 and above or in those showing early signs of cognitive decline. Furthermore, the study did not include a group of young adults, so we were not able to assess group differences relative to younger participants to determine the age specificity of our results. However, our study included a longitudinal aspect, which accounts for individuals' cognitive performance 7 years after baseline and implies that some of the links we report are related to within-subject modification. Finally, 2 min of EEG resting-state recording might not be deemed enough to optimally characterize the ongoing brain state. Recent studies showed however that resting-state brain activity allows the robust differentiation of individuals from brain recordings as short as 30 s, ushering in the notion of a neural fingerprint [21].

rsFC variability, long considered as noise, has been identified as a key marker of age-related cognitive variability in several BOLD signal MRI studies [33], whereas its characterization through EEG remains underexplored, limiting our understanding of its electrophysiological underpinnings in aging. Here, we reported a diurnal pattern of dynamic SN, CEN, DMN rsFC associated with baseline cognitive performance, longitudinal cognitive trajectories, and pathological markers, which differ when

*Published in : GeroScience (2025)*
*DOI: 10.1007/s11357-025-01974-2*
*Status : Postprint (Author's version)*

considering theta or gamma band, suggesting that these two rhythms have specific and opposite roles in cognitive functioning and AD pathology. In the theta band, greater stability in network integration was associated with better memory performance, suggesting that a well-maintained connectivity structure supports efficient long-range communication. In contrast, in the gamma band, greater fluctuations in network integration were linked to better executive and attentional function, indicating that these cognitive abilities benefit from more flexible connectivity patterns. These findings highlight that neither stability nor flexibility is inherently beneficial; their effects depend on the underlying frequency band and cognitive function involved. More broadly, our findings suggest that diurnal rsFC dynamics may parallel aging-related changes in brain function, offering a compressed timescale representation of the aging process. The association between cognitive performance and diurnal network dynamics parallels the long-term increase in network integration observed in aging, often interpreted as an adaptive response to declining neural efficiency [53]. Investigating rsFC dynamics within the CEN, DMN, and SN on a diurnal scale, as described in the triple network model [55], provides new insights into cognitive aging.

Taken together, our findings support the promises of diurnal rsFC variability as a marker of cognitive functioning in aging. They also highlight the value of temporal multilayer network approaches using EEG time-frequency data in capturing subtle brain activity long before cognitive changes in aging. Future research should refine these findings and explore their clinical applications, particularly for identifying early markers of neurodegeneration.

## Acknowledgements

This research was not preregistered and did not receive any specific grant from funding agencies in the public, commercial, or not-for-profit sectors. Data collection was conducted at the GIGA-In Vivo Imaging platform of ULiège, Belgium. Data sharing for this project was provided by the GIGA-CRC Human Imaging. Data access can be provided upon reasonable request to FC and GV.

## Author contributions

Conceptualization: KB, FC, GVa, TH. Methodology: KB, ACG, JBP, FC, GVa, TH. Investigation: KB, CP, CB, FC, GVa, TH. Supervision: KB, FE, GVa, TH. Writing—original draft: KB, TH. Writing—review and editing: KB, ACG, JBP, GVo, FE, CP, CB, FC, GVa, TH.

## Funding

Funding for this project was provided by Fonds National de la Recherche Scientifique (FRS-FNRS, FRSM 3.4516.11, F.4513.17, and T.0242.19, EOS Project MEMODYN No. 30446199; Belgium), the Wallonia-Brussels Federation (Grant for Concerted Research Actions—SLEEPDEM 17/27–09), Stop Alzheimer Foundation (Belgium, grants 15018, 2019/0025), University of Liège, Fondation Simone et Pierre Clerdent, European Regional Development Fund (ERDF, Radiomed Project). [18F]Flutemetamol doses

were provided and cost covered by GE Healthcare Ltd (Little Chalfont, UK) as part of an investigator-sponsored study (ISS290) agreement. This agreement had no influence on the protocol and results of the study reported here. JBP and ACG were supported by the Swedish Research Council (#2022-01108), the Swedish Alzheimer Foundation (#AF-968323), a Consolidator Karolinska Institute grant, the Swedish Brain Foundation (FO2022-0147), Gamla Tjänarinnor (#2020-01016; #202101207; #2022-01341), KI foundations, Stohnes or the project "A Multimodal Brain Connectivity Marker for the Early Detection of Alzheimer's Disease" funded by the European Union – NextGenerationEU and the Romanian Government, under the National Recovery and Resilience Plan for Romania, contract no. 760250/28.12.2023, cod PNRR-C9-I8-CF109/31.07.2023, through the Romanian Ministry of Research, Innovation and Digitalization, within Component 9, Investment I8.

# Declarations

## CONFLICT OF INTEREST

The authors declare no competing interests.

# References

1. Anderson ND, Craik FIM. 50 years of cognitive aging theory. J Gerontol B Psychol Sci Soc Sci. 2017;72(1):1–6. https://doi.org/10. 1093/geronb/gbw108.
2. Andrews-Hanna JR, Reidler JS, Sepulcre J, Poulin R, Buckner RL. Functional-anatomic fractionation of the brain's default network. Neuron. 2010;65(4):550–62. https://doi.org/10.1016/j.neuron.2010.02.005.
3. Babiloni C, Blinowska K, Bonanni L, Cichocki A, De Haan W, Del Percio C, et al. What electrophysiology tells us about Alzheimer's disease: a window into the synchronization and connectivity of brain neurons. Neurobiol Aging. 2020;85:58–73. https://doi.org/10.1016/j.neurobiolaging.2019.09.008.
4. Bakhtiari A, Petersen J, Urdanibia-Centelles O, Ghazi MM, Fagerlund B, Mortensen EL, et al. Power and distribution of evoked gamma oscillations in brain aging and cognitive performance. Geroscience. 2023;45(3):1523–38.
5. Başar E, Düzgün A. How is the brain working? Int J Psychophysiol. 2016;103:3–11. https://doi.org/10.1016/j.ijpsycho.2015.02.007.
6. Bassett DS, Wymbs NF, Porter MA, Mucha PJ, Carlson JM, Grafton ST. Dynamic reconfiguration of human brain networks during learning. Proc Natl Acad Sci U S A. 2011;108(18):7641–6.
7. Bassett DS, Yang M, Wymbs NF, Grafton ST. Learning-induced autonomy of sensorimotor systems. Nat Neurosci. 2015;18(5):744–51. https://doi.org/10.1038/nn.3993.
8. Benjamini Y, Hochberg Y. Controlling the false discovery rate: a practical and powerful approach to multiple testing. J R Stat Soc Series B Stat Methodol. 1995;57(1):289–300. https://doi.org/10.1111/j.2517-6161.1995.tb02031.x.
9. Bennis K, Eustache F, Collette F, Vandewalle G, & Hinault T. Daily dynamics of resting-state EEG theta and gamma fluctuations are associated with cognitive performance in healthy aging. J Gerontol B Psychol Sci Soc Sci, 2024;gbae152. https://doi.org/10.1093/geronb/gbae152
10. Blautzik J, Vetter C, Peres I, Gutyrchik E, Keeser D, Berman A, et al. Classifying fMRI-derived resting-state connectivity patterns according to their daily rhythmicity. Neuroimage. 2013;71:298–306. https://doi.org/10.1016/j.neuroimage.2012.08.010.
11 . Cabeza R, Albert M, Belleville S, Craik FIM, Duarte A, Grady CL, et al. Maintenance, reserve and compensation: the cognitive neuroscience of healthy ageing. Nat Rev Neurosci. 2018;19(11):701–10. https://doi.org/10.1038/s41583-018-0068-2.
12. Calhoun VD, Miller R, Pearlson G, Adalı T. The chronnectome: time-varying connectivity networks as the next frontier in fMRI data discovery. Neuron. 2014;84(2):262–74. https://doi.org/10.1016/j.neuron.2014.10.015.
13. Canal-Garcia A, Veréb D, Mijalkov M, Westman E, Volpe G, Pereira JB. Dynamic multilayer functional connectivity detects preclinical and clinical Alzheimer's disease. Cereb Cortex. 2024. https://doi.org/10.1093/cercor/bhad542.
14. Chan MY, Alhazmi FH, Park DC, Savalia NK, Wig GS. Resting-state network topology differentiates task signals across the adult life span. J Neurosci. 2017;37(10):2734– 45. https://doi.org/10.1523/JNEUROSCI.2406-16.2017.

*Published in : GeroScience (2025)*
*DOI: 10.1007/s11357-025-01974-2*
*Status : Postprint (Author's version)*

15. Chand GB, Wu J, Hajjar I, Qiu D. Interactions of the salience network and its subsystems with the default-mode and the central-executive networks in normal aging and mild cognitive impairment. Brain Connect. 2017;7(7):401–12. https://doi.org/10.1089/brain.2017.0509.
16. Chang Y-W, Zufiria-Gerbolés B, Gómez-Ruiz E, Canal-Garcia A, Zhao H, Mijalkov M, et al. BRAPH 2: a flexible, open-source, reproducible, community-oriented, easy-to-use framework for network analyses in neurosciences. bioRxiv. https://doi.org/10.1101/2025.04.11.648455
17. Chen AC, Oathes DJ, Chang C, Bradley T, Zhou ZW, Williams LM, et al. Causal interactions between frontoparietal central executive and default-mode networks in humans. Proc Nat Acad Sci.n2013;110(49):19944–9. https://doi.org/10.1073/pnas.1311772110.
18. Chylinski DO, Van Egroo M, Narbutas J, Grignard M, Koshmanova E, Berthomier C, et al. Heterogeneity in the links between sleep arousals, amyloid-β, and cognition. JCI Insight. 2021;6(24):e152858. https://doi.org/10.1172/jci.insight.152858.
19. Chylinski D, Van Egroo M, Narbutas J, Muto V, Bahri MA, Berthomier C, et al. Timely coupling of sleep spindles and slow waves linked to early amyloid-β burden and predicts memory decline. Elife. 2022;11:e78191. https://doi.org/10.7554/eLife.78191.
20. Courtney SM, Hinault T. When the time is right: temporal dynamics of brain activity in healthy aging and dementia. Prog Neurobiol. 2021;203:102076. https://doi.org/10.1016/j.pneurobio.2021.102076.
21. Da Silva Castanheira J, Orozco Perez HD, Misic B, Baillet S. Brief segments of neurophysiological activity enable individual differentiation. Nat Commun. 2021;12(1):5713. https://doi.org/10.1038/s41467-021-25895-8.
22. Damoiseaux JS. Effects of aging on functional and structural brain connectivity. Neuroimage. 2017;160:32–40. https://doi.org/10.1016/j.neuroimage.2017.01.077.
23. Desikan RS, Ségonne F, Fischl B, Quinn BT, Dickerson BC, Blacker D, et al. An automated labeling system for subdividing the human cerebral cortex on MRI scans into gyral based regions of interest. Neuroimage. 2006;31(3):968–80. https://doi.org/10.1016/j.neuroimage.2006.01.021.
24. Drinkenburg W (Pim), Tok S, Ahnaou A. Functional neurophysiological biomarkers of early-stage alzheimer's disease: an experimental perspective of network hyperexcitability in disease progression and pharmacological interventions. Alzheimer's & Dementia. 2022;18(S4):e060269. https://doi.org/10.1002/alz.060269.
25. Droby A, Varangis E, Habeck C, Hausdorff JM, Stern Y, Mirelman A, et al. Effects of aging on cognitive and brain inter-network integration patterns underlying usual and dual-task gait performance. Front Aging Neurosci. 2022;14:956744.
26. Facer-Childs ER, Campos BM, Middleton B, Skene DJ, Bagshaw AP. Circadian phenotype impacts the brain's resting-state functional connectivity, attentional performance, and sleepiness. Sleep. 2019;42(5):zsz033. https://doi.org/10.1093/sleep/zsz033.
27. Farahani FV, Karwowski W, D'Esposito M, Betzel RF, Douglas PK, Sobczak AM, et al. Diurnal variations of resting-state fMRI data: a graph-based analysis. Neuroimage. 2022;256:119246. https://doi.org/10.1016/j.neuroimage.2022.119246.
28 . Fell J, Axmacher N. The role of phase synchronization in memory processes. Nat Rev Neurosci. 2011;12(2):105–18. https://doi.org/10.1038/nrn2979.
29. Ferreira LK, Busatto GF. Resting-state functional connectivity in normal brain aging. Neurosci Biobehav Rev. 2013;37(3):384-400. https://doi.org/10.1016/j.neubiorev.2013.01.017.
30. Finnigan S, Robertson IH. Resting EEG theta power correlates with cognitive performance in healthy older adults: resting theta EEG correlates with cognitive aging. Psychophysiology. 2011;48(8):1083–7. https://doi.org/10.1111/j.1469-8986.2010. 01173.x.
31. Fischl B. FreeSurfer. Neuroimage. 2012;62(2):774–81. https://doi.org/10.1016/j.neuroimage.2012.01.021.
32. Gaggioni G, Ly JQM, Muto V, Chellappa SL, Jaspar M, Meyer C, Delfosse T, Vanvinckenroye A, Dumont R, Coppieters 'T Wallant D, Berthomier C, Narbutas J, Van Egroo M, Luxen A, Salmon E, Collette F, Phillips C, Schmidt C, & Vandewalle G. Age-related decrease in cortical excitability circadian variations during sleep loss and its links with cognition. Neurobiol Aging. 2019;78:52–63. https://doi.org/10.1016/j.neurobiolaging.2019.02.004
33. Garrett DD, Kovacevic N, McIntosh AR, Grady CL. The importance of being variable. J Neurosci. 2011;31(12):4496–503. https://doi.org/10.1523/JNEUROSCI.5641-10.2011.
34. Golchert J, Smallwood J, Jefferies E, Seli P, Huntenburg JM, Liem F, et al. Individual variation in intentionality in the mind-wandering state is reflected in the integration of the default-mode, fronto-parietal, and limbic networks. Neuroimage. 2017;146:226–35. https://doi.org/10.1016/j.neuroimage.2016.11.025.
35. Gramfort A, Papadopoulo T, Olivi E, Clerc M. OpenMEEG: opensource software for quasistatic bioelectromagnetics. BioMed Eng OnLine. 2010;9(1):45. https://doi.org/10.1186/1475-925X-9-45.
36. Guzmán-Vélez E, Diez I, Schoemaker D, Pardilla-Delgado E, Vila-Castelar C, Fox-Fuller JT, et al. Amyloid-β and tau pathologies relate to distinctive brain dysconnectomics in preclinical autosomal-dominant Alzheimer's disease. Proc Natl Acad Sci U S A. 2022;119(15):e2113641119. https://doi.org/10.1073/pnas.2113641119.
37. He L, Wang X, Zhuang K, Qiu J. Decreased dynamic segregation but increased dynamic integration of the resting-state functional networks during normal aging. Neuroscience. 2020;437:54–63. https://doi.org/10.1016/j.neuroscience.2020.04.030.
38. Hinault T, Mijalkov M, Pereira JB, Volpe G, Bakke A, Courtney SM. Age-related differences in network structure and dynamic synchrony of cognitive control. Neuroimage. 2021;236:118070. https://doi.org/10.1016/j.neuroimage.2021.118070.
39. Hinault T, Baillet S, Courtney SM. Age-related changes of deep-brain neurophysiological activity. Cereb Cortex. 2023;33(7):3960–8. https://doi.org/10.1093/cercor/bhac319.
40 . Jauny G, Eustache F, Hinault T. Connectivity dynamics and cognitive variability during aging. Neurobiol Aging. 2022;118:99–105. https://doi.org/10.1016/j.neurobiolaging.2022.07.001.

*Published in : GeroScience (2025)*
*DOI: 10.1007/s11357-025-01974-2*
*Status : Postprint (Author's version)*

41. Jensen O, Gips B, Bergmann TO, Bonnefond M. Temporal coding organized by coupled alpha and gamma oscillations prioritize visual processing. Trends Neurosci. 2014;37(7):357–69. https://doi.org/10.1016/j.tins.2014.04.001.
42. Jockwitz C, Caspers S. Resting-state networks in the course of aging—differential insights from studies across the lifespan vs. amongst the old. Pflugers Arch. 2021;473(5):793–803. https://doi.org/10.1007/s00424-021-02520-7.
43. Khazaie H, Veronese M, Noori K, Emamian F, Zarei M, Ashkan K, et al. Functional reorganization in obstructive sleep apnoea and insomnia: a systematic review of the resting-state fMRI. Neurosci Biobehav Rev. 2017;77:219–31. https://doi.org/10.1016/j.neubiorev.2017.03.013.
44. Koen JD, Rugg MD. Neural dedifferentiation in the aging brain. Trends Cogn Sci. 2019;23(7):547–59. https://doi.org/10.1016/j.tics.2019.04.012.
45. Kumral D, Şansal F, Cesnaite E, Mahjoory K, Al E, Gaebler M, et al. BOLD and EEG signal variability at rest differently relate to aging in the human brain. Neuroimage. 2020;207:116373. https://doi.org/10.1016/j.neuroimage.2019.116373.
46. Kryger MH, Roth T, & Dement WC. Principles and practice of sleep medicine E-book: expert consult-online and print. Elsevier Health Sciences; 2010.
47. La Corte V, Piolino P. Episodic foresight in normal cognitive and pathological aging. Gériatrie et Psychologie Neuropsychiatrie du Viellissement. 2016;14(1):58–66. https://doi.org/10.1684/pnv.2016.0594.
48. La Corte V, Sperduti M, Malherbe C, Vialatte F, Lion S, Gallarda T, et al. Cognitive decline and reorganization of functional connectivity in healthy aging: the pivotal role of the salience network in the prediction of age and cognitive performances. Front Aging Neurosci. 2016;8:204. https://doi.org/10.3389/fnagi.2016.00204.
49. Lopez ME, Aurtenetxe S, Pereda E, Cuesta P, Castellanos NP, Bruna R, et al. Cognitive reserve is associated with the functional organization of the brain in healthy aging: A MEG study. Front Aging Neurosci. 2014;6. https://doi.org/10.3389/fnagi.2014.00125.
50. Lundqvist M, Herman P, Warden MR, Brincat SL, Miller EK. Gamma and beta bursts during working memory readout suggest roles in its volitional control. Nat Commun. 2018;9(1):394. https://doi.org/10.1038/s41467-017-02791-8.
51. Ly JQM, Gaggioni G, Chellappa SL, Papachilleos S, Brzozowski A, Borsu C, et al. Circadian regulation of human cortical excitability. Nat Commun. 2016;7(1):11828. https://doi.org/10.1038/ncomms11828.
52. Ma J, Kim M, Kim J, Hong G, Namgung E, Park S, et al. Decreased functional connectivity within the salience network after two-week morning bright light exposure in individuals with sleep disturbances: a preliminary randomized controlled trial. Sleep Med. 2020;74:66–72. https://doi.org/10.1016/j.sleep.2020.05.009.
53. Malagurski B, Liem F, Oschwald J, Mérillat S, Jäncke L. Longitudinal functional brain network reconfiguration in healthy aging. Hum Brain Mapp. 2020;41(17):4829–45. https://doi.org/10.1002/hbm.25161.
54. Mattar MG, Cole MW, Thompson-Schill SL, Bassett DS. A functional cartography of cognitive systems. PLoS Comput Biol. 2015;11(12):e1004533. https://doi.org/10.1371/journal.pcbi.1004533.
55. Menon V. Large-scale brain networks and psychopathology: a unifying triple network model. Trends Cogn Sci. 2011;15(10):483-506.
56. Menon V, Palaniyappan L, Supekar K. Integrative brain network and salience models of psychopathology and cognitive dysfunction in schizophrenia. Biol Psychiatry. 2023;94(2):108–20. https://doi.org/10.1016/j.biopsych.2022.09.029.
57. Mijalkov M, Kakaei E, Pereira JB, Westman E, Volpe G. BRAPH: a graph theory software for the analysis of brain connectivity. PLoS ONE. 2017;12(8):e0178798. https://doi.org/10.1371/journal.pone.0178798.
58. Miraglia F, Vecchio F, Rossini PM. Searching for signs of aging and dementia in EEG through network analysis. Behav Brain Res. 2017;317:292–300. https://doi.org/10.1016/j.bbr.2016.09.057.
59. Missonnier P, Herrmann FR, Michon A, Fazio-Costa L, Gold G, Giannakopoulos P. Early disturbances of gamma band dynamics in mild cognitive impairment. J Neural Transm. 2010;117(4):489–98. https://doi.org/10.1007/s00702-010-0384-9.
60. Mucha PJ, Richardson T, Macon K, Porter MA, Onnela J-P. Community structure in time-dependent, multiscale, and multiplex networks. Science. 2010;328(5980):876–8. https://doi.org/10.1126/science.1184819.
61. Murdock MH, Yang CY, Sun N, et al. Multisensory gamma stimulation promotes glymphatic clearance of amyloid. Nature. 2024;627:149–56. https://doi.org/10.1038/s41586-024-07132-6.
62. Narbutas J, Van Egroo M, Chylinski D, Bahri MA, Koshmanova E, Talwar P, et al. Associations between cognitive complaints, memory performance, mood, and amyloid-β accumulation in healthy amyloid negative latemidlife individuals. J Alzheimers Dis. 2021;83(1):127–41. https://doi.org/10.3233/JAD-210332.
63. Ng KK, Lo JC, Lim JKW, Chee MWL, Zhou J. Reduced functional segregation between the default mode network and the executive control network in healthy older adults: a longitudinal study. Neuroimage. 2016;133:321–30. https://doi.org/10.1016/j.neuroimage.2016.03.029.
64. Oschmann M, Gawryluk JR, Alzheimer's Disease Neuroimaging Initiative. A longitudinal study of changes in resting-state functional magnetic resonance imaging functional connectivity networks during healthy aging. Brain Connect. 2020;10(7):377–84. https://doi.org/10.1089/brain.2019.0724.
65. Pascual-Marqui RD, Michel CM, Lehmann D. Low resolution electromagnetic tomography: a new method for localizing electrical activity in the brain. Int J Psychophysiol. 1994;18(1):49–65. https://doi.org/10.1016/0167-8760(84)90014-X.
66. Pedersen M, Zalesky A, Omidvarnia A, Jackson GD. Multilayer network switching rate predicts brain performance. Proc Natl Acad Sci U S A. 2018;115(52):13376–81. https://doi.org/10.1073/pnas.1814785115.

*Published in : GeroScience (2025)*
*DOI: 10.1007/s11357-025-01974-2*
*Status : Postprint (Author's version)*

67. Pishdadian S, Hoang NV, Baker S, Moscovitch M, Rosenbaum RS. Not only memory: investigating the sensitivity and specificity of the mnemonic similarity task in older adults. Neuropsychologia. 2020;149:107670. https://doi.org/10.1016/j.neuropsychologia.2020.107670.
68. Puxeddu MG, Faskowitz J, Betzel RF, Petti M, Astolfi L, Sporns O. The modular organization of brain cortical connectivity across the human lifespan. Neuroimage. 2020;218:116974. https://doi.org/10.1016/j.neuroimage.2020.116974.
69. Raichle ME. The brain's default mode network. Annu Rev Neurosci. 2015;38:433–47. https://doi.org/10.1146/annurev-neuro-071013-014030.
70. Reuter-Lorenz PA, Park DC. How does it STAC up? Revisiting the scaffolding theory of aging and cognition. Neuropsychol Rev. 2014;24(3):355–70. https://doi.org/10.1007/s11065-014-9270-9.
71. Rizzolo L, Narbutas J, Van Egroo M, Chylinski D, Besson G, Baillet M, et al. Relationship between brain AD biomarkers and episodic memory performance in healthy aging. Brain Cogn. 2021;148:105680. https://doi.org/10.1016/j.bandc.2020.105680.
72. Rodrigue KM, Kennedy KM, Park DC. Beta-amyloid deposition and the aging brain. Neuropsychol Rev. 2009;19(4):436–50. https://doi.org/10.1007/s11065-009-9118-x.
73. Sala-Llonch R, Bartrés-Faz D, Junqué C. Reorganization of brain networks in aging: A review of functional connectivity studies. Front Psychol. 2015;6. https://doi.org/10.3389/fpsyg.2015.00663.
74. Setton R, Mwilambwe-Tshilobo L, Girn M, Lockrow AW, Baracchini G, Hughes C, et al. Age differences in the functional architecture of the human brain. Cereb Cortex. 2022;33(1):114–34. https://doi.org/10.1093/cercor/bhac056.
75. Sporns O. Graph theory methods: applications in brain networks. Dialogues Clin Neurosci. 2018;20(2):111–21. https://doi.org/10.31887/DCNS.2018.20.2/osporns.
76. Stam CJ, Nolte G, Daffertshofer A. Phase lag index: assessment of functional connectivity from multi channel EEG and MEG with diminished bias from common sources. Hum Brain Mapp. 2007;28(11):1178–93. https://doi.org/10.1002/hbm.20346.
77. Stanley ML, Simpson SL, Dagenbach D, Lyday RG, Burdette JH, Laurienti PJ. Changes in brain network efficiency and working memory performance in aging. PLoS ONE. 2015;10(4):e0123950.
78. Stark SM, Yassa MA, Lacy JW, Stark CE. A task to assess behavioral pattern separation (BPS) in humans: Data from healthy aging and mild cognitive impairment. Neuropsychologia. 2013;51(12):2442–9. https://doi.org/10.1016/j.neuropsychologia.2012.12.014.
79. Tadel F, Baillet S, Mosher JC, Pantazis D, Leahy RM. Brainstorm: a user-friendly application for MEG/EEG analysis. Comput Intell Neurosci. 2011;2011:1–13. https://doi.org/10.1155/2011/879716.
80. Thomas Yeo BT, Krienen FM, Sepulcre J, Sabuncu MR, Lashkari D, Hollinshead M, et al. The organization of the human cerebral cortex estimated by intrinsic functional connectivity. J Neurophysiol. 2011;106(3):1125–65. https://doi.org/10.1152/jn.00338.2011.
81. Toppi J, Astolfi L, Risetti M, Anzolin A, Kober SE, Wood G. Different topological properties of EEG-derived networks describe working memory phases as revealed by graph theoretical analysis. Front Hum Neurosci. 2018;11:637. https://doi.org/10.3389/fnhum.2017.00637.
82. Tzourio-Mazoyer N, Landeau B, Papathanassiou D, Crivello F, Etard O, Delcroix N, et al. Automated anatomical labeling of activations in SPM using a macroscopic anatomical parcellation of the MNI MRI single-subject brain. Neuroimage. 2002;15(1):273–89. https://doi.org/10.1006/nimg.2001.0978.
83. Uddin LQ. Bring the noise: reconceptualizing spontaneous neural activity. Trends Cogn Sci. 2020;24(9):734–46. https://doi.org/10.1016/j.tics.2020.06.003.
84. Uddin LQ, Yeo BTT, Spreng RN. Towards a universal taxonomy of macro-scale functional human brain networks. Brain Topogr. 2019;32(6):926–42. https://doi.org/10.1007/s10548-019-00744-6.
85. Van Egroo M, Chylinski D, Narbutas J, Besson G, Muto V, Schmidt C, et al. Early brainstem [18F]THK5351 uptake is linked to cortical hyperexcitability in healthy aging. JCI Insight. 2021;6(2):e142514. https://doi.org/10.1172/jci.insight.142514.
86. Van Egroo M, Narbutas J, Chylinski D, Villar González P, Ghaemmaghami P, Muto V, et al. Preserved wakedependent cortical excitability dynamics predict cognitive fitness beyond age-related brain alterations. Commun Biol. 2019;2(1):449. https://doi.org/10.1038/s42003-019-0693-y.
87. Varangis E, Habeck CG, Razlighi QR, Stern Y. The effect of aging on resting state connectivity of predefined networks in the brain. Front Aging Neurosci. 2019;11:234. https://doi.org/10.3389/fnagi.2019.00234.
88. Wig GS. Segregated systems of human brain networks. Trends Cogn Sci. 2017;21(12):981–96. https://doi.org/10.1016/j.tics.2017.09.006.